

Thermo-optical properties and nonlinear optical response of smectic liquid crystals containing gold nanoparticles

P. B. de Melo,¹ A. M. Nunes,² L. Omena,¹ S. M. S. do Nascimento,¹ M. G. A. da Silva,²
M. R. Meneghetti,² and I. N. de Oliveira¹

¹*Instituto de Física, Universidade Federal de Alagoas 57072-970 Maceió-AL, Brazil*

²*Instituto de Química e Biotecnologia, Universidade Federal de Alagoas 57072-970 Maceió-AL, Brazil*

(Received 1 August 2015; published 15 October 2015)

The present work is devoted to the study of the thermo-optical and nonlinear optical properties of smectic samples containing gold nanoparticles with different shapes. By using the time-resolved Z-scan technique, we determine the effects of nanoparticle addition on the critical behavior of the thermal diffusivity and thermo-optical coefficient at the vicinity of the smectic-*A*-nematic phase transition. Our results reveal that introduction of gold nanoparticles affects the temperature dependence of thermo-optical parameters, due to the local distortions in the orientational order and heat generation provided by guest particles during the laser exposure. Further, we show that a nonlinear optical response may take place at temperatures where the smectic order is well established. We provide a detailed discussion of the effects associated with the introduction gold nanoparticles on the mechanisms behind the thermal transport and optical nonlinearity in liquid-crystal samples.

DOI: [10.1103/PhysRevE.92.042504](https://doi.org/10.1103/PhysRevE.92.042504)

PACS number(s): 61.30.Eb, 42.70.Df, 64.70.M-, 47.57.J-

I. INTRODUCTION

Over the past decade, the development of new soft materials based on liquid crystals has attracted remarkable interest due to their large applicability in several areas, such as photonic [1] and biotechnology [2,3]. In particular, a rich phenomenology has been observed in liquid crystals samples containing colloidal particles, where the nature of guest-host interactions and the emergence of elastic distortions constitute the main mechanisms behind the enhanced electro-optical responses [4] and the formation of self-organized structures [5] in the resulting systems. Indeed, different long-range interactions may take place among micron-sized particles dispersed in liquid-crystalline environments as a response to the elastic distortions in the orientational order [6,7], which depend on the strength and direction of the anchoring at the colloid surface [7–9]. Such effective elastic-induced interactions can be reasonably explored to produce artificial colloidal structures exhibiting regular geometric patterns as desired in many photonic applications [5,10]. However, a distinct scenario is observed when the guest particles present a diameter around a few tens of nanometers, being too small to induce macroscopic distortions in the orientational order [4,11]. As a consequence, guest-host interactions play a predominant role in the thermal and optical behavior of the system, with the addition of nanoparticles emerging as an excellent alternative to improve physical properties of liquid-crystalline samples, such as the nematic temperature range [12] and the Fréedericksz transition threshold [11].

Recently, several works have been devoted to the study of liquid crystal systems doped with gold nanoparticles (NPs) [4,13–24]. The main reason is that such nanoparticles exhibit interesting optical and electrical properties associated with the surface plasmon resonance, which can be tuned by adjusting their size, shape, and concentration [25]. In fact, the introduction of gold NPs in liquid-crystalline materials has been successfully used to obtain hybrid systems with novel electro-optical properties that explore the sensitive of the surface plasmon resonance to the director orientation and

the amplitude of an external field [4,13,15,22]. A prominent example is that reorientation of the nematic order can be used as an effective mechanism to induce and control the long-range orientational order of gold nanorods dispersed in liquid crystals, giving rise to collective plasmonic effects in the optical properties of the hybrid system [4,24]. Concerning effects associated with an external field, it has been reported that nematic samples containing gold NPs present a lower Fréedericksz threshold voltage than pure one, due to the increase of the dielectric anisotropy [26,27]. In ferroelectric liquid crystals, the addition of gold NPs leads to an enhancement in the optical tilt and the emergence of memory effects even in the limit of low operating voltages, resulting from the plasmon-induced increase of the local electric field around the guest particles [28].

A stable dispersion of gold nanoparticles in liquid-crystalline environments depends on their size and aspect ratio, reflecting the anchoring conditions provided by the surface functionalization of the nanoparticles during their synthesis procedure [18,21,24]. As a consequence, thermal and hydrodynamical properties of liquid crystals samples containing gold NPs exhibit a rich phenomenology associated with the interplay of the host anisotropy and the geometric shape of guest nanoparticles [18,21,24,29,30]. In particular, a strong anisotropy has been observed in the translational diffusion coefficients of anisotropic gold nanoparticles with respect to the uniform far-field director in nematic liquid crystals, which is governed by the equilibrium alignment of the colloids and the local particle-induced distortion of the orientational order [21]. Further, measurements of the thermal-induced optical nonlinearity revealed that a crossover from self-focusing to self-defocusing behavior may take place depending on the shape of nanoparticles dispersed in the nematic samples, with the nonlinear optical response of the system being reasonably tuned by an external magnetic field [23].

Although nematic liquid crystals doped with gold NPs have been widely studied, only a few works have been devoted to the investigation of gold dispersion in smectic samples [16,17]. For nanospheres presenting a diameter larger than

smectic layer spacing, atomic force micrography revealed that the layered structure and elasticity of smectic phase prevent the irreversible aggregation of gold nanoparticles, giving rise to a stable dispersion in such a phase [16]. On the other hand, a self-assembly of gold nanospheres takes place in the smectic phase at the regime of high concentrations [17]. In particular, it is observed the emergence of linear or curved arrays with micron-scaled periodicities, which depend on the cell geometry. Such results show that nanoscale dispersions in smectic samples exhibit a rich phenomenology associated with the one-dimensional quasi-long-range positional order. However, the effects of gold nanoparticles shape on thermal and optical properties of the smectic liquid crystals have not been investigated so far.

In this work, we study the thermo-optical and nonlinear optical properties of smectic samples containing gold NPs, close to the smectic-A–nematic phase transition. By using the time-resolved Z-scan technique, we determine the effects of NPs addition on the temperature dependence of the thermal diffusivity and thermo-optical coefficient in the smectic sample. Our results shows that the critical behavior of the thermo-optical parameters is sensitive to the shape of gold NPs, with the local distortions in the orientational order and heat generation by the guest particles playing an important role in the heat diffusion in the liquid crystal host. Further, the analysis of the position dependence of the normalized transmittance reveals that a nonlinear optical response may take place at temperatures where the smectic order is well established. The mechanisms behind the heat transport and the optical nonlinearity in smectic samples are analyzed, giving emphasis to the effects associated with the introduction gold NPs.

II. MATERIALS AND METHODS

We chose the compound 4-octyl-4'-cyanobiphenyl (8CB) as our liquid crystal sample. It presents an isotropic-nematic phase transition at $T_{NI} = 313.5$ K and a nematic–smectic-A transition at $T_{AN} = 306.5$ K. This compound exhibits a good chemical stability upon laser exposure and it was purchased from Sigma-Aldrich, being used without further purification. Gold nanorods were prepared in aqueous solution by the seed-mediated method [31], with cetyltrimethylammonium bromide (CTAB) as the capping agent. Gold nanospheres were obtained in a toluene solution by a two-phase liquid-liquid system [32] by using dodecanethiol as the capping agent. The nanoparticles were redispersed in toluene and then transferred to the liquid crystal sample in the isotropic phase. Surfactants used as capping agents stayed stable during the exchange of solvents and subsequent transfer process to the liquid crystal, with a homeotropic anchoring being expected at the colloid surface. In order to obtain well-separated guest particles, the studied nanoparticles were dispersed in 8CB at a low weight concentration ($c = 0.02$ wt.%), where no visible aggregates were observed in the resultant system.

Homeotropic samples were prepared by treating cleaned glass surfaces with surfactant. Spacers were used to maintain the cell thickness at $\ell_0 = 100$ μm . The cells were filled by capillarity action in the isotropic phase of 8CB ($T \approx 323$ K) and slowly cooled down to room temperature. Samples were observed under a crossed-polarized microscope to ensure

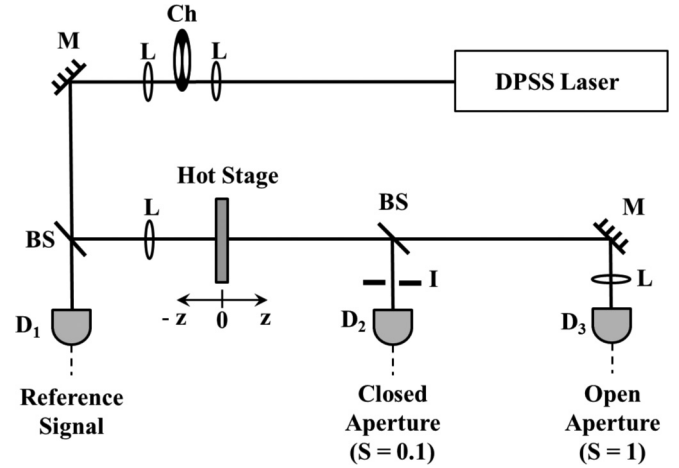


FIG. 1. Schematic representation of the experimental setup: L, lens; BS, beam splitter; I, iris; M, mirror; Ch, chopper; D, detector.

alignment and uniformity. Further, the extinction spectra of filled cells at room temperature were recorded using a ultraviolet-visible spectrometer (Lambda 1050, Perkin-Elmer). Samples were placed in a temperature-controlled oven within the accuracy of 0.1 K, with the sample temperature being varied in steps of $\Delta T = 0.2$ K, in a rate of 0.1 K/min. After reaching the target temperature, the measurement was performed after a waiting time of 20 min in order to certify that the system has reached the equilibrium configuration.

In order to investigate the thermo-optical and nonlinear optical properties of gold NPs dispersion in smectic liquid crystals, we employed the time-resolved Z-scan technique using a linear polarized CW diode-pumped solid state (DPSS) laser at $\lambda = 532$ nm as the light source. The laser beam presented a Gaussian profile with a well-defined vertical polarization and the laser power used to excite the sample was $P = 0.6$ – 2.5 mW. The laser beam was focused by a lens with a focal length of 15 cm, which provided a minimum waist of $w_0 = 42$ μm , resulting in a confocal distance $z_c = 10.6$ mm. A mechanical chopper was used to modulate the laser beam, producing square-wave pulses with a duration of 70 ms. The sample was excited at normal incidence in order to avoid reorientation of the orientational order. The sample was moved back and forth along the z axis around the minimum beam waist of the laser during the measurement, with a single displacement step of 5 mm. By using an iris centered along the beam propagation direction, the far-field transmittance was measured as a function of the position z of the sample. Controlling the iris aperture, S , we were able to analyze the distortions of beam wavefront associated with two distinct effects [33,34]: (i) thermal-induced variation of the refractive index (closed aperture, $S = 0.1$) and (ii) nonlinear optical absorption (open aperture, $S = 1$). A schematic representation of the experimental setup is shown in Fig. 1.

III. MODEL BACKGROUND

A. Thermal lens

It is well established that thermal properties of low absorbing liquid crystal samples can be reasonably investigated using

the time-resolved Z-scan technique, which is a sensitive and efficient method to measure the thermal lens effect [35–37]. Such an effect consists of the conversion of the absorbed energy into heat when a Gaussian laser beam passes through the sample, which behaves itself as a lenslike optical element due to the temperature-induced change in the optical path. In particular, a self-focusing or defocusing behavior in the beam center is observed due to the local heating and modification of the liquid crystal birefringence. The formation time of the thermal lens can be also used to determine the thermal diffusivity of the sample [35]. The optical path change due to thermal lens effect may be described by the aberration model [38], with the transient intensity in the far field given by

$$I(\tau) = I(0) \left\{ 1 - \frac{\theta}{2} \tan^{-1} \left[\frac{2\gamma}{(3 + \gamma^2) + (9 + \gamma^2) \left(\frac{\tau_c}{2\tau} \right)} \right] \right\}^2, \quad (1)$$

with $\gamma = z/z_c$, where z is the sample position in relation to the position of minimum beam waist ($z = 0$) and z_c is the confocal parameter. θ is the thermal-induced phase shift of the beam wavefront after its passage through the sample. τ is the exposure time of the sample during each square pulse, while τ_c is the characteristic time for the formation of the thermal lens. The parameters τ_c and θ can be directly obtained from the fitting of the experimental data for the transient transmittance by using Eq. (1). θ and τ_c are free parameters which can be associated with the sample and experimental setup parameters as follows [37,38]

$$\theta = - \left[\frac{P_i A \ell_0}{\kappa \lambda} \right] \frac{dn_o}{dT} \quad (2)$$

and

$$\tau_c = \frac{w^2}{4D}. \quad (3)$$

Here w is the beam waist at the sample, defined as $w = w_0 \sqrt{1 + \gamma^2}$, and D is the thermal diffusivity. P_i is the incident laser power, A is the absorption coefficient at the excitation wavelength, and κ is the thermal conductivity. n_o is the ordinary refractive index of the liquid crystal samples.

B. Nonlinear optical absorption

As we have described before, the Z-scan technique is a sensitive method to measure distortions in the beam wavefront caused by refractive and absorptive nonlinearities of the sample. In an experimental configuration where a fully open aperture is used, such a technique becomes insensitive to the effects associated with a pure refractive nonlinearity [33]. As a consequence, one can extract the absorptive nonlinearity from variation of the far-field transmittance as the sample is moved around the position of minimum beam waist ($z = 0$). For a Gaussian beam, the dependence of the normalized transmittance, \bar{T} , on the sample position along the z axis can be expressed by:

$$\bar{T}(z) \approx 1 - \frac{\beta I_0 L_{\text{eff}}}{8^{1/2} [1 + (z/z_0)^2]}, \quad (4)$$

where β is the nonlinear absorption coefficient, I_0 is the incident intensity, and $L_{\text{eff}} = (1 - e^{-\alpha \ell_0})/\alpha$, with α being

the linear absorption coefficient. It is important to stress that Eq. (4) holds for $\beta I_0 L_{\text{eff}} \ll 1$. The origin of the absorptive nonlinearity may be associated with saturation of the single-photon absorption ($\beta < 0$) or multiphoton absorption ($\beta > 0$). In particular, the phenomenon of the saturable nonlinear absorption is characterized by a symmetric transmittance profile exhibiting maximum at $z = 0$, while the multiphoton absorption is marked by a symmetric transmittance profile exhibiting minimum at $z = 0$. In what follows, we will use the above description to analyze the effects of the addition of gold nanoparticle on the thermo-optical and nonlinear optical properties of smectic liquid crystals.

IV. RESULTS

In Fig. 2 we show the TEM images and extinction spectra of 8CB samples containing gold nanoparticles with distinct geometric shapes. The analysis of TEM images revealed that gold nanorods present an average length $L = 40$ nm, with an aspect ratio around $r = 2.5$, as shown in Fig. 2(a). Further, one can observe that the gold nanorods present a certain alignment which can be associated with a reduction of the local distortion in the orientational order. In fact, previous works have demonstrated that nanorods may exhibit distinct alignments with respect to the far-field nematic director, depending on

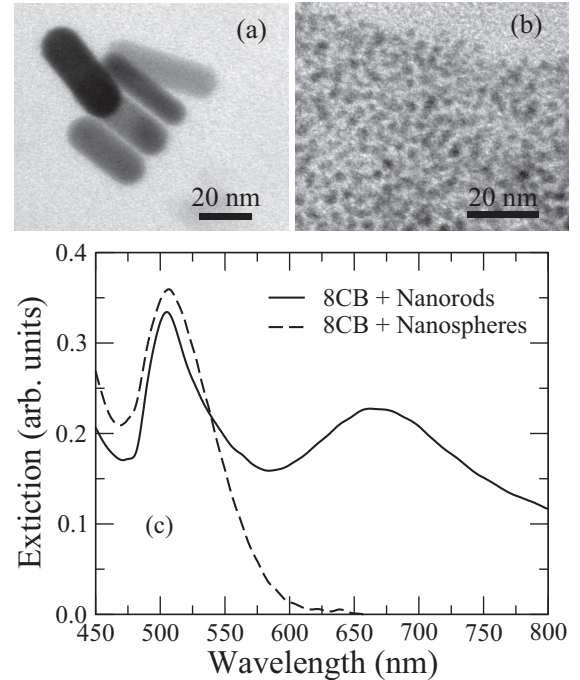


FIG. 2. TEM images of liquid crystals samples containing gold nanoparticles of different shapes: (a) nanorods and (b) nanospheres. Gold nanorods exhibit an average length of 40 nm and an aspect ratio of 2.5, while the nanospheres present an average diameter of 4 nm. (c) Extinction spectra of nanorods (solid line) and nanospheres (dashed line) of gold dispersed in the 8CB host, confined in a homeotropic cell. Notice the transversal plasmon band ($\lambda_t = 507$ nm) has a higher extinction than the longitudinal plasmon band ($\lambda_l = 669$ nm), indicating that the gold nanorods are aligned parallel to the far-field nematic director.

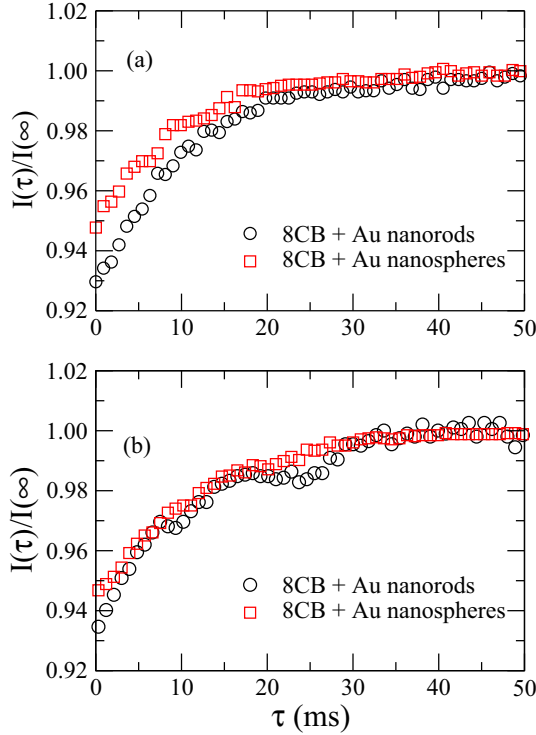


FIG. 3. (Color online) Transient intensities of 8CB liquid crystal containing gold nanorods (black circles) and nanospheres (red squares) at distinct reduced temperatures: (a) $t = 0.004$ (nematic phase) and (b) $t = -0.004$ (smectic phase). In all cases, the nanoparticles concentration was $c = 0.02$ wt%. One can note that the thermal lens phenomenon is less pronounced in the smectic phase, with the thermal-induced distortion in the beam wave front and the characteristic time to the formation of the thermal lens being sensitive to the nanoparticles shape.

the nature and strength of anchoring at the colloid surface [21]. In Fig. 2(b), it is observed that the gold nanospheres are uniformly dispersed in the 8CB sample, exhibiting an average diameter $D = 4$ nm. It is important to stress that such nanospheres and nanorods present dimensions larger than the smectic layer spacing of 8CB, $d = 3.3$ nm. The extinction spectra of 8CB samples containing gold nanoparticles in homeotropic cells are exhibited in Fig. 2(c), where typical surface plasmon resonances can be observed. In both cases, extinction spectra were recorded at $T = 300$ K, well below to the nematic–smectic-*A* transition temperature. The spectrum of gold nanorods dispersion presents two bands centered at $\lambda_t = 507$ nm and $\lambda_l = 669$ nm, which correspond respectively to transversal and longitudinal surface plasmon resonances [25]. Further, we notice that the transversal plasmon band has a higher extinction than the longitudinal plasmon band, indicating that the gold nanorods are aligned parallel to the far-field nematic director [4,21]. Concerning the dispersion of gold nanospheres, the extinction spectrum presents a single band centered at $\lambda_t = 507$ nm that is associated with transversal plasmon resonance.

In order to investigate the effects of nanoparticles shape on the thermo-optical properties of liquid crystal samples, we present in Fig. 3 the time evolution of the far-field

transmittance through a closed aperture, with $S = 0.1$. The transient transmittances were recorded for samples placed at the post focal position $z = \sqrt{3}z_c$, with the concentration of gold nanospheres and nanorods being $c = 0.02$ wt%. The measurements were performed at different reduced temperatures $t = [T - T_{AN}]/T_{AN}$, where T_{AN} is the nematic–smectic-*A* transition. At the nematic phase ($t > 0$), we observe that doped samples exhibit a self-focusing behavior characterized by the increase of the transient intensity during the exposure time, as shown in Fig. 3(a). One can notice that the self-focusing of the laser beam is more pronounced in the sample containing nanorods, with the transient intensity presenting a slow relaxation to the steady state. In particular, different characteristic times to the formation of the thermal lens are observed, indicating that the shape of gold nanoparticles plays an important role in the thermal transport of doped samples in the nematic phase. Indeed, previous works have reported that the translational diffusion of colloids in a nematic liquid crystal is sensitive to their geometric shape [21], which can be a determinant feature to the thermal transport once gold nanoparticles behave as heat sources during the laser exposure. A distinct scenario is observed in the smectic phase ($t < 0$), where the relaxation of the transient intensity to the steady state does not appear to be substantially dependent on the shape of nanoparticles. Such a result shows that the geometry of the gold nanoparticles does not induce a significant modification in the mean free path of hydrodynamic modes responsible for the heat diffusion in the smectic phase. Further, a small reduction in the self-focusing behavior is observed in the smectic phase, with the thermal-induced distortions in the beam wave front being slightly higher in the sample containing nanorods.

The analysis of the time evolution of the far-field transmittance can be suitably used to obtain the physical parameters associated with the formation of a thermal lens in liquid crystal samples. By using the aberration lens model, we have computed the thermal-induced phase shift and the thermal diffusivity of the liquid-crystalline materials from the fitting of transient intensities. In Fig. 4, we show the thermal-induced phase shift in the beam wave front, θ , at the vicinity of the nematic–smectic-*A* phase transition of 8CB samples containing gold nanorods and nanospheres. The phase shifts were rescaled by the power of the incident laser beam in order to allow a better analysis of the photothermal process. We observe that the beam phase shift exhibits a deep valley at the nematic–smectic-*A* transition temperature that is more evident in the sample containing gold nanorods. As defined in Eq. (2), the temperature dependence of the beam phase shift reflects the thermal behavior of ordinary refractive index at the regime of normal incidence [37], which can be directly associated with the orientational order parameter [39]. Although small anomalies in the orientational order parameter and its temperature derivatives are expected due to the thermal fluctuations at the vicinity of T_{AN} [40], the present results show that the introduction of nanoparticles affects significantly the variation rate of the ordinary refractive index with temperature at the nematic–smectic-*A* phase transition. Indeed, strong changes in the refractive indices take place during the laser exposure of the sample, which are associated with the heat generation from the nonradiative decaying of the plasmon excitation in the guest particles [23,41,42]. Such a heating tends to disturb

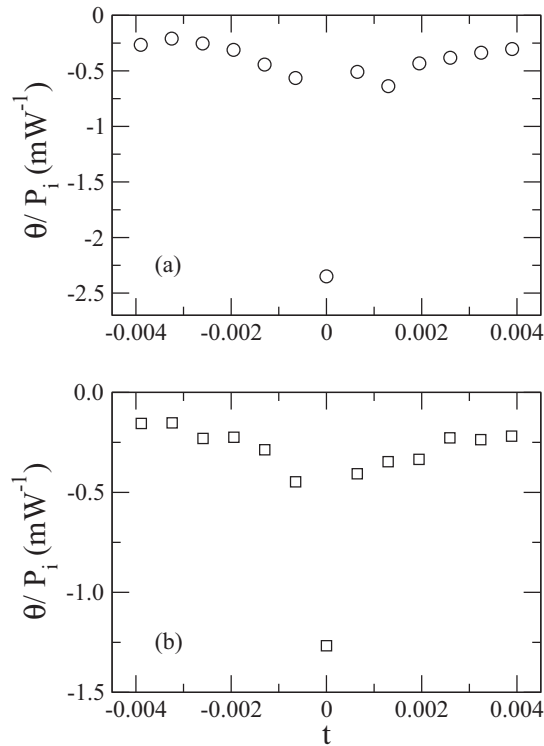


FIG. 4. Beam phase shift in units of the incident laser power as a function of the reduced temperature for 8CB samples containing (a) gold nanorods and (b) gold nanospheres at a concentration of 0.02 wt%. One can observe a sharp drop in the thermal-induced phase shift at the nematic–smectic-*A* transition temperature, which is more pronounced in the 8CB sample doped with gold nanorods.

the orientational order around the nanoparticles, becoming more relevant close to the transition temperature due to the long-range correlations. Further, the beam phase shift seems to be sensitive to the nanoparticles shape, presenting a higher absolute value in liquid crystals doped with gold nanorods even far from the transition temperature. This behavior may be associated with average alignment of gold nanorods along the far-field nematic director, favoring the excitation of transversal plasmons and the heat transport perpendicular to the director.

In Fig. 5, we present the thermal diffusivity of 8CB samples as a function of the reduced temperature for distinct morphologies of gold nanoparticles: (a) nanorods and (b) nanospheres. One can note that the thermal diffusivity exhibits the typical vanishing behavior at the nematic–smectic-*A* phase transition [37,43], presenting a slight dependence on the shape of gold nanoparticles. We notice that the vanishing behavior is less pronounced in the sample doped with gold nanospheres, indicating that the thermodynamic response functions may be sensitive to the shape of guest nanoparticles. It is important to stress that the reduction of the thermal diffusivity reflects the divergence of the specific heat at the transition temperature, while the thermal conductivity stays finite [43]. Previous works have shown that the introduction of nonmesogenic impurities may give rise to a random disorder in liquid crystal samples, leading to a suppression of the peak of the specific heat at the nematic–smectic-*A* phase transition as the concentration of nonmesogenic solute is increased [44]. In our case, the cap

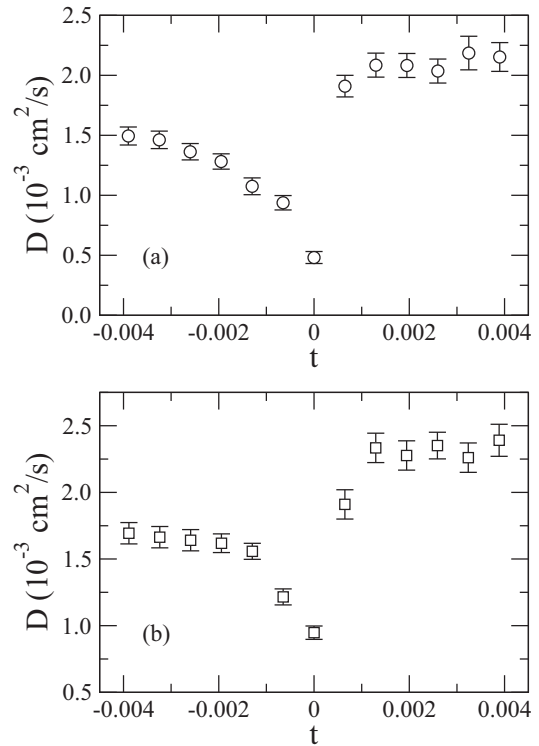


FIG. 5. Temperature dependence of the thermal diffusivity of 8CB samples doped with (a) gold nanorods and (b) gold nanospheres. The concentration of gold nanoparticles in 8CB samples was $c = 0.02$ wt%. Notice that the thermal diffusivity exhibits a vanishing critical behavior at the nematic–smectic-*A* phase transition, with the heat diffusion being governed by short-range processes that depend on the nanoparticle shape.

agent induces a strong homeotropic anchoring at the surface of gold nanospheres, which behave as sources of random disorder due to the orientational distortions with respect to the far-field director. Although similar local distortions in the orientational order are also expected around the gold nanorods, the absorption spectrum reveals that such nanoparticles tend to align along the direction defined by the far-field director. As a consequence, the effects associated with the distortions in nematic ordering tend to be minimized in the sample containing gold nanorods, with the peak suppression of the specific heat at the phase transition being less pronounced than in the liquid crystal doped with gold nanospheres. Far from transition temperature, it is observed that the thermal diffusivity presents a larger value in the 8CB containing nanospheres in nematic and smectic phases. Such result is related to the fact of translational diffusion and the effective surface area are larger for nanospheres, favoring the heat diffusion through the sample.

It must be emphasized that a random disorder resulting from the introduction of nonmesogenic impurities may also lead to memory effects and a reduction in the transition temperatures in liquid-crystalline systems, especially in the regime of high concentrations [37,44,45]. Although a small variation in the critical vanishing behavior of the thermal diffusivity has been observed, we have not found evidence of memory effects in the thermo-optical properties of doped

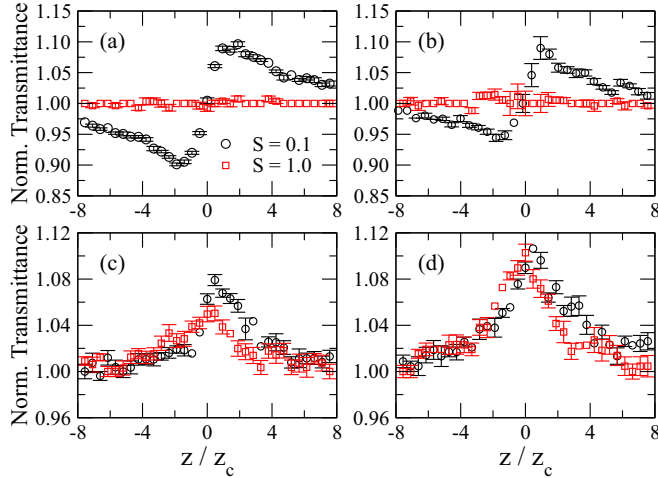


FIG. 6. (Color online) Normalized Z-scan transmittance of 8CB doped gold nanorods at different reduced temperatures: (a) $t = 0.003$, (b) $t = -0.003$, (c) $t = -0.013$, and (d) $t = -0.014$. The measurements were performed in the configurations of closed (black circles) and open (red squares) apertures. Here we observe that a nonlinear absorption takes place as the temperature is diminished well below to the nematic–smectic-*A* transition temperature.

samples upon heating and cooling processes. Further, the analysis of polarized optical microscopy images revealed that the nematic–smectic-*A* transition temperature is reduced by 0.1 K in samples containing gold nanoparticles. This small variation in the transition temperature lies within the error tolerance of the experimental setup and it may not reflect the effects of a random disorder induced by nonmesogenic impurities. The absence of such phenomena may be associated with the very low concentration of gold nanoparticles in the liquid-crystalline system, which was kept constant in $c = 0.02$ wt.%. This behavior is consistent with previous experimental studies reporting that the nematic–smectic-*A* transition temperature does not change significantly for small concentrations of gold nanoparticles [16,46]

Finally, we analyze the emergence of nonlinear effects on the optical properties due to the addition of gold nanoparticles. In Fig. 6, we present the position dependence of the normalized transmittance of 8CB sample containing gold nanorods at distinct reduced temperatures. Z-scan measurements were performed in the configurations of closed ($S = 0.1$) and ($S = 1.0$) open apertures. In the nematic phase ($t = 0.003$), we observe that the normalized transmittance in the closed aperture configuration exhibits a typical Z-scan curve for the thermal lens phenomenon in a medium presenting $dn_o/dT < 0$, with the minimum and maximum responses occurring in $z = -\sqrt{3}z_c$ and $z = \sqrt{3}z_c$, respectively. Further, the normalized transmittance in the open aperture configuration stays constant, indicating that the distortions in the beam wave front are only associated with the thermal lens phenomenon. Such behavior persists in the smectic-*A* phase ($t = -0.003$) close to the transition temperature, where no significant modification can be observed in the normalized transmittance for closed and open configurations of the Z-scan experimental setup, as shown in Fig. 6(b). A different scenario takes place in the smectic-*A* phase well below to the transition temperature

($t = -0.013$), as one can observe in Fig. 6(c). In the closed aperture configuration, the valley-peak Z-scan signature in the normalized transmittance is replaced by a curve presenting a maximum close to $z = 0$. This result shows the emergence of a distinct contribution to the distortion of the beam wave front besides the thermal lens phenomenon. In fact, we observe that a nonlinear absorption signature appears in the normalized transmittance for measurements realized in the open aperture configuration. More specifically, we notice that such absorptive nonlinearity is associated with a saturation of the single-photon absorption of the transversal plasmon band, being characterized by $\beta < 0$. As the sample temperature is reduced ($t = -0.014$), the effects of the nonlinear absorption becomes more pronounced, as exhibited in Fig. 6(d). Concerning the 8CB sample containing gold nanospheres, we have not observed any signal associated with the emergence of an absorptive nonlinearity along the range of temperatures investigated (not shown), indicating that the thermal lens is the predominant phenomenon in this sample.

It is important to stress that the absorptive nonlinearity emerges in the doped sample at the smectic-*A* phase, once the smectic-*A*–crystal phase transition in 8CB occurs at $t = -0.035$. Although a thermal-induced nonlinear optical response has been previously explored in nematic liquid crystals doped with gold nanoparticles [23,42], the present results seem to be the first report of a saturable absorption phenomenon associated with the interplay between the smectic ordering and the anisotropic shape of gold nanorods. In particular, the emergence of an absorptive nonlinearity indicates that the smectic layered structure affects the orientational and spatial distribution of colloidal particles through the sample. Indeed, the presence of guest particles tends to induce the formation of dislocations as the layered structure emerges [16]. As a consequence, a self-organization process may take place in order to reduce the high energy cost associated with the distortions in the smectic order. As the temperature is reduced, the equilibrium configuration may favor the alignment of elongated nanoparticles, giving rise to a saturation in the linear absorption of plasmon bands. A similar behavior has been observed in polymeric films, where an enhanced absorptive nonlinearity is obtained from the nanorods alignment induced by the film stretching [47]. By using Eq. 4, we have estimated the nonlinear absorption coefficient from the fitting of the normalized transmittance, with $\beta \approx -2 \times 10^{-3}$ cm/W. This value is at least three orders of magnitude higher than that reported in a large variety of soft materials, such as polymers [47] and colloidal dispersions of metallic nanoparticles [48,49].

V. SUMMARY AND CONCLUSIONS

In summary, we have studied the effects of gold nanoparticles in the thermal and nonlinear optical properties of smectic crystals. Using the time-resolved Z-scan technique, we computed the thermal diffusivity and beam phase shift from the far-field transient intensities. Our results showed that thermo-optical properties of liquid crystals are sensitive to the geometric shape of the guest particles in the vicinity of the nematic–smectic-*A* phase transition. It is observed that the introduction of gold nanospheres tends to suppress the

typical vanishing behavior of thermal diffusivity at the phase transition. This suppression is associated with the emergence of a random disorder in the nematic ordering [43], which is induced by local distortions around guest particles presenting a homeotropic anchoring at their surface [4]. The modification in the critical behavior is observed to be less pronounced in samples containing elongated nanoparticles, although similar disorder has been expected in 8CB samples containing gold nanorods. However, the elongated shape of nanoparticles minimizes the nematic distortions due to their alignment along the far-field nematic director, reducing the disorder effects on the critical behavior of the thermal diffusivity. Further, we showed that the beam phase shift exhibits a deep valley at the nematic–smectic-*A* transition temperature that is more evident in the sample containing gold nanorods. In fact, gold nanoparticles behave as heat generators during the laser exposure, disturbing the orientational order around them and giving rise to strong changes in the temperature dependence of the refractive indices. At temperatures where the smectic order is well established, we observed that an absorptive nonlinearity emerges in 8CB liquid crystal doped with nanorods, which is absent in the sample containing nanospheres. Such a result is the first report of a nonlinear optical phenomenon associated with the interplay between the smectic ordering and the anisotropic shape of gold nanorods. In particular, it is expected that a self-organization process takes place in order to reduce the high energy cost associated with the

distortions in the smectic order [16], favoring the alignment of elongated nanoparticles and giving rise to a saturation in the linear absorption of plasmon bands [47]. Despite the fact that the Z-scan technique is a sensitive experimental setup to probe changes in the molecular and colloidal organization of the sample investigated, additional methods are required to assert the spatial distribution and the relative orientation of gold nanorods in relation to the far-field nematic orientation in the smectic phase, such as atomic force microscopy [16] and imaging by two-photon luminescence [18]. Our findings show that the introduction of gold nanoparticles in smectic samples provides a rich phenomenology associated with the distortions in the layered structure and self-organization of guest particles, which may motivated future theoretical and experimental investigations. From a practical point of view, the present results open the possibility of new applications based on smectic liquid crystals containing nanomaterials, as optical limiting and sensor protection [50].

ACKNOWLEDGMENTS

We are grateful to M. L. Lyra for useful discussions. This work was partially supported by Instituto Nacional de Ciência e Tecnologia de Fluidos Complexos (INCT-FCx), CAPES, CNPq/MCT, FAPEAL, and FINEP (Brazilian Research Agencies).

-
- [1] A. C. Edrington, A. M. Urbas, P. DeRege, C. X. Chen, T. M. Swager, N. Hadjichristidis, M. Xenidou, L. J. Fetters, J. D. Joannopoulos, Y. Fink, and E. L. Thomas, *Adv. Mater.* **13**, 421 (2001).
- [2] T. Araki and H. Tanaka, *J. Phys.: Condens. Matter* **18**, 193 (2006).
- [3] V. K. Gupta, J. J. Skaife, T. B. Dubrovsky, and N. L. Abbott, *Science* **279**, 2077 (1998).
- [4] Q. Liu, Y. Yuan, and I. I. Smalyukh, *Nano Lett.* **14**, 4071 (2014).
- [5] I. Mušević, M. Škarabot, U. Tkalec, M. Ravnik, and S. Žumer, *Science* **313**, 954 (2006).
- [6] H. Stark, *Phys. Rep.* **351**, 387 (2001).
- [7] I. I. Smalyukh, O. D. Lavrentovich, A. N. Kuzmin, A. V. Kachynski, and P. N. Prasad, *Phys. Rev. Lett.* **95**, 157801 (2005).
- [8] K. Takahashi, M. Ichikawa, and Y. Kimura, *Phys. Rev. E* **77**, 020703(R) (2008).
- [9] J. I. Fukuda, H. Stark, M. Yoneya, and H. Yokoyama, *Phys. Rev. E* **69**, 041706 (2004).
- [10] M. Škarabot, M. Ravnik, S. Žumer, U. Tkalec, I. Poberaj, D. Babič, N. Osterman, and I. Mušević, *Phys. Rev. E* **77**, 031705 (2008).
- [11] M. Kaczmarek, O. Buchnev, and I. Nandhakumar, *Appl. Phys. Lett.* **92**, 103307 (2008).
- [12] F. Li, O. Buchnev, C. I. Cheon, A. Glushchenko, V. Reshetnyak, Y. Reznikov, T. J. Sluckin, and J. L. West, *Phys. Rev. Lett.* **97**, 147801 (2006).
- [13] J. Müller, C. Sönnichsen, H. von Poschinger, G. von Plessen, T. A. Klar, and J. Feldmann, *Appl. Phys. Lett.* **81**, 171 (2002).
- [14] K. C. Chu, C. Y. Chao, Y. F. Chen, Y. C. Wu, and C. C. Chen, *Appl. Phys. Lett.* **89**, 103107 (2006).
- [15] L.-H. Hsu, K.-Y. Lo, S.-A. Huang, C.-Y. Huang, and C.-S. Yang, *Appl. Phys. Lett.* **92**, 181112 (2008).
- [16] R. Pratibha, W. Park, and I. I. Smalyukh, *J. Appl. Phys.* **107**, 063511 (2010).
- [17] J. Milette, S. Relaix, C. Lavigne, V. Toader, S. J. Cowling, I. M. Saez, R. B. Lennox, J. W. Goodby, and L. Reven, *Soft Matter* **8**, 6593 (2012).
- [18] Q. Liu, B. Senyuk, J. Tang, T. Lee, J. Qian, S. He, and I. I. Smalyukh, *Phys. Rev. Lett.* **109**, 088301 (2012).
- [19] J. S. Pendery, O. Merchiers, D. Coursault, J. Grand, H. Ayeb, R. Greget, B. Donnio, J.-L. Gallani, C. Rosenblatt, N. Féliidj, Y. Borensztein, and E. Lacaze, *Soft Matter* **9**, 9366 (2013).
- [20] M. Infusino, A. D. Luca, F. Ciuchi, A. Ionescu, N. Scaramuzza, and G. Strangi, *J. Mater. Sci.* **49**, 1805 (2013).
- [21] B. Senyuk, D. Glugla, and I. I. Smalyukh, *Phys. Rev. E* **88**, 062507 (2013).
- [22] G. B. Hadjichristov, Y. G. Marinov, A. G. Petrov, E. Bruno, L. Marino, and N. Scaramuzza, *J. Appl. Phys.* **115**, 083107 (2014).
- [23] A. Acreman, M. Kaczmarek, and G. D’Alessandro, *Phys. Rev. E* **90**, 012504 (2014).
- [24] Q. Liu, J. Tang, Y. Zhang, A. Martinez, S. Wang, S. He, T. J. White, and I. I. Smalyukh, *Phys. Rev. E* **89**, 052505 (2014).
- [25] M. A. Garcia, *J. Phys. D* **44**, 283001 (2011).
- [26] H. Qi, B. Kinkead, and T. Hegmann, *Adv. Funct. Mater.* **18**, 212 (2008).
- [27] S. Khatua, P. Manna, W.-S. Chang, A. Tcherniak, E. Friedlander, E. R. Zubarev, and S. Link, *J. Phys. Chem. C* **114**, 7251 (2010).

- [28] S. Kaur, S. P. Singh, A. M. Biradar, Amit Choudhary, and K. Sreenivas, *Appl. Phys. Lett.* **91**, 023120 (2007).
- [29] B. Senyuk, J. S. Evans, P. J. Ackerman, T. Lee, P. Manna, L. Vigderman, E. R. Zubarev, J. van de Lagemaat, and I. I. Smalyukh, *Nano Lett.* **12**, 955 (2012).
- [30] H. Qi and T. Hegmann, *ACS Appl. Mater. Interfaces* **1**, 1731 (2009).
- [31] M. G. A. da Silva, A. M. Nunes, S. M. P. Meneghetti, and M. R. Meneghetti, *C. R. Chimie* **16**, 640 (2013).
- [32] M. Brust, M. Walker, D. Bethell, D. J. Schiffrin, and R. Whyman, *J. Chem. Soc., Chem. Commun.*, 801 (1994).
- [33] M. Sheik-Bahae, A. A. Said, T.-H. Wei, D. J. Hagan, and E. W. van Stryland, *IEEE J. Quantum Electron.* **26**, 760 (1990).
- [34] C. Jacinto, D. N. Messias, A. A. Andrade, S. M. Lima, M. L. Baesso, and T. Catunda, *J. Non-Cryst. Solids* **352**, 3582 (2006).
- [35] N. M. Kimura, A. de Campos, P. A. Santoro, M. Simões, S. L. Gómez, and A. J. Palangana, *Phys. Lett. A* **370**, 173 (2007).
- [36] J. R. D. Pereira, A. M. Mansanares, A. J. Palangana, and M. L. Baesso, *Phys. Rev. E* **64**, 012701 (2001).
- [37] L. Omena, P. B. de Melo, M. S. S. Pereira, and I. N. de Oliveira, *Phys. Rev. E* **89**, 052511 (2014).
- [38] C. A. Carter and J. M. Harris, *Appl. Opt.* **23**, 476 (1984).
- [39] J. Li, S. Gauza, and S.-T. Wu, *J. Appl. Phys.* **96**, 19 (2004).
- [40] M. C. Çetinkaya, S. Yildiz, H. Özbek, P. Losada-Pérez, J. Leys, and J. Thoen, *Phys. Rev. E* **88**, 042502 (2013).
- [41] S. Kubo, A. Diaz, Y. Tang, T. S. Mayer, I. C. Khoo, and T. E. Mallouk, *Nano Lett.* **7**, 3418 (2007).
- [42] D. Lysenko, E. Ouskova, S. Ksondzyk, V. Reshetnyak, L. Cseh, G. H. Mehl, and Y. Reznikov, *Eur. Phys. J. E* **35**, 33 (2012).
- [43] M. Marinelli, F. Mercuri, U. Zammit, and F. Scudieri, *Phys. Rev. E* **58**, 5860 (1998).
- [44] M. Marinelli, A. K. Ghosh, and F. Mercuri, *Phys. Rev. E* **63**, 061713 (2001).
- [45] A. Ranjkesh, M. Ambrožič, S. Kralj, and T. J. Sluckin, *Phys. Rev. E* **89**, 022504 (2014).
- [46] P. Oswald, J. Milette, S. Relaix, L. Reven, A. Dequidt, and L. Lejcek, *Europhys. Lett.* **103**, 46004 (2013).
- [47] J. Li, S. Liu, Y. Liu, Fei Zhou, and Z.-Y. Li, *Appl. Phys. Lett.* **96**, 263103 (2010).
- [48] J. Olesiak-Banska, M. Gordel, R. Kolkowski, K. Matczyszyn, and Marek Samoc, *J. Phys. Chem. C* **116**, 13731 (2012).
- [49] M. Hari, S. Mathew, B. Nithyaja, S. A. Joseph, V. P. N. Nampoori, and P. Radhakrishnan, *Opt. Quantum Electron.* **43**, 49 (2012).
- [50] I. C. Khoo, M. V. Wood, M. Y. Shih, and P. H. Chen, *Opt. Express* **4**, 432 (1999).